Proceedings of the IASS 2024 Symposium
Redefining the Art of Structural Design
August 26-30, 2024, Zurich Switzerland
Philippe Block, Giulia Boller, Catherine DeWolf,
Jacqueline Pauli, Walter Kaufmann (eds.)

Topology Optimization of Active Tensegrity Structures

Yafeng WANG*, Xian XU, Yaozhi LUO

College of Civil Engineering and Architecture, Zhejiang University
866 Yuhangtang Road, Hangzhou, Zhejiang 310058, China
*yafengwang@zju.edu.cn

Abstract

This study investigates the optimum design of active tensegrity structures through topology optimization. Due to the integration of the active control system, the topology design of active tensegrity structures is different from passive tensegrity structures. The member topology and actuator layout are considered as binary design variables in the optimization and their coupling relation is handled by auxiliary constraints. The member cross-sectional areas, prestress, and control strategies (i.e., actuator length changes) are treated as continuous variables and designed simultaneously. The equilibrium condition, member yielding, cable slackness, strut buckling, and the limitations on the nodal displacements as well as other practical requirements are formulated as constraints. Typical benchmark examples indicate that the active designs obtained through the proposed topology optimization method can significantly decrease structure mass compared with conventional active tensegrity designs and thus leading to more lightweight tensegrity structures.

Keywords: topology optimization; active tensegrity structure; mixed integer programming; lightweight structures

1. Introduction

Tensegrity structures are self-stressed pin-jointed systems consisting of cables and struts that only carry axial forces. Appropriate initial selfstress needs to be introduced into a tensegrity structure to maintain its stable equilibrium. Due to their unique characteristics, tensegrity systems have been widely applied in many engineering and scientific fields [1–3].

Mass-efficiency is one of the main advantages of tensegrity structures because the members only need to carry axial forces thus have a better performance in terms of material utilization. Generally, tensegrity structures have a high stiffness-to-weight ratio and for this reason have been applied to design lightweight structures and tremendes methods have been proposed to minimize the weight/mass of tensegrity structures [4–6]. Most applications and design methods of lightweight tensegrity structures focus on passive tensegrity systems, i.e., all the members in the system are passive and not be capable of changing their length actively to react to external loads. The structural members of passive tensegrity structures cannot change their lengths actively and thus have to passively resist external loads. Active tensegrity structures are equipped with actuators to actively adapt the internal forces and nodal positions and thus can actively resist external loads. It has been verified that active tensegrity structures can use less material compared to passive tensegrity structures [7]. Existing studies on active tensegrity structure optimum design only focus on sizing and/or shape optimization, i.e., the structural element topology does not change during the design process, which vastly limits the design space and the improvement of mass-saving structural performance.

This paper aims to develop a general framework for the topology design of minimal mass active tensegrity structures. Both the parameters relating to the structural system (e.g., prestress and member cross-sectional areas) and the structural topology (e.g., member connectivities and actuator layout) are

incorporated and designed simultaneously. The member topology and actuator layout are considered as binary design variables in the optimization and their coupling relation is handled by auxiliary constraints. The member cross-sectional areas, prestress, and control strategies (i.e., actuator length changes) are treated as continuous variables and designed simultaneously. The equilibrium condition, member yielding, cable slackness, strut buckling, and the limitations on the nodal displacements as well as other practical requirements are formulated as constraints. Typical benchmark examples indicate that the active designs obtained through the proposed topology optimization method can significantly decrease the material consumption compared with the equivalent topology-optimized passive designs and thus leading to more lightweight tensegrity structures.

2. Basic Formulations for Active Tensegrity Structures

Without loss of generality, an active tensegrity structure with *n* nodes and *m* members equipped with *c* actuators in a three-dimensional Cartesian space is considered. *E* is used to denote the set of the indices of members in the structure and E_i is used to denote the set of the indices of members connecting to node *i*. *C* and *S* are used to denote the sets of the indices of cables and struts, respectively. n^f is used to denote the number of free degrees of freedom (DOFs). Y_i, ρ_i, a_i, and l_i are used to denote the material Young's modules, material density, cross-sectional area, and length of member *i*, respectively.

2.1 Initial self-stress

Tensegrity structures are self-equilibrated systems consisting of tensile cables and compression struts. To maintain a equilibrium state, the initial prestress $\mathbf{F}^0 \in \mathbb{R}^{m\times 1}$ in the structure should satisfy

$$\mathbf{A}\mathbf{F}^0 = \mathbf{0} \tag{1}$$

where $\mathbf{A} \in \mathbb{R}^{n^f \times m}$ is the equilibrium matrix of the structure [8]. To ensure member unilateral rigidity (i.e., cables in tension and struts in compression) in *prestress state*, $\mathbf{F}^0$ should satisfy

$$\begin{cases} F_i^0 > 0, & \forall i \in C \\ F_i^0 < 0, & \forall i \in S \end{cases} \tag{2}$$

Note that for a kinematically indeterminate tensegrity system, in addition to Eq. (1) the prestress should also ensure it be capable of stiffening all the internal mechanism modes [9].

2.2 Equilibrium and compatibility

Under a given nodal load $\mathbf{P} \in \mathbb{R}^{n^f \times 1}$, the equilibrium of the tensegrity structure can be expressed as

$$\mathbf{A}\mathbf{F} = \mathbf{P} + \mathbf{P}^s \tag{3}$$

where $\mathbf{P}^s \in \mathbb{R}^{m\times 1}$ is the self-weight load and $\mathbf{F}$ is the member internal force vector caused by nodal loading. The member force $\mathbf{F} \in \mathbb{R}^{m\times 1}$ is related by the member elastic elongation $\mathbf{e} \in \mathbb{R}^{m\times 1}$ according to the constitutive law as

$$\mathbf{F} = \mathbf{B}\mathbf{e} \tag{4}$$

According to the compatibility condition, the relation between the nodal displacement $\mathbf{u}$, the member elastic elongation $\mathbf{e}$, and the member active elongation $\Delta\mathbf{L} \in \mathbb{R}^{m\times 1}$ is given by

$$\mathbf{A}^{\mathrm{T}}\mathbf{u} = \mathbf{e} + \Delta\mathbf{L} \tag{5}$$

Substituting Eq. (5) into Eq. (4) gives

$$\mathbf{F} = \mathbf{B}\left(\mathbf{A}^{\mathrm{T}}\mathbf{u} - \Delta\mathbf{L}\right) \tag{6}$$

where $\mathbf{B} \in \mathbb{R}^{m \times m}$ is the diagonal member stiffness matrix given by $\mathbf{B} = \mathrm{diag}\left(\frac{Y_i a_i}{l_i}\right)$. Note that, similar to the nodal displacements, member force **F** in Eq. (6) can be divided into two parts which correspond to the effects of external load **P** and the effects of actuation, respectively. In addition, **F** in Eq. (6) only denotes the part of the member force caused by the external load **P** and the effects of actuation; the total member force should also include the prestress $\mathbf{F}^0$.

2.3 Structure mass and self-weight

The mass of an active tensegrity structure is denoted as *M* which is composed of two parts: the mass of members M_m and the mass of actuators M_a, i.e.,

$$M = M_m + M_a \tag{7}$$

The mass of members can be determined by

$$M_m = \sum_{i \in E} \rho_i l_i a_i \tag{8}$$

The mass of an actuator usually depends on its actuation force capacity, i.e., the maximum actuation force it can resist. The mass of an actuator is assumed proportional to its actuation force capacity. The actuation force capacity of the i^{th} actuator is denoted as F_i, and then the mass of the actuators can be expressed as

$$M_a = \sum_{i \in E_a} c F_i \tag{9}$$

where E_a denotes the set of the indices of the actuators; and *c* is the proportional factor which takes the value of 0.1kg/kN according to [10].

Assume the weight of members and actuators are transformed into equivalent nodal loads. The weight of a member and the actuator installed on it is assumed to be evenly distributed to the two nodes it connects. Therefore, the weight applied to the i^{th} node can be determined by

$$W_i = \frac{1}{2}\left(\sum_{j \in E_i} \rho_j l_j a_j + c \sum_{j \in E_a \cap E_i} F_j \right) g \tag{10}$$

where *g* is the gravity and takes a value of 9.8 N/kg.

3. Topology Optimization Model

As introduced in Section 2, the topology optimization is carried out based on ground structure method, hence the formulations in Section 3 should also be expressed in terms of the whole ground structure. The key point to make this modification is that the candidate members in the ground structure may be unnecessary to form the final structure, and these unnecessary members should be ensured to have zero cross-sectional areas and forces in the optimization. In addition, some parameters such as *C*, *S*, and E_a are unknown in advance hence the corresponding formulations should be re-expressed in the optimization. In the following content, *E* and E_i are used to respectively denote the sets of the indices of all the candidate members and the members connecting to node *i* in the ground structure.

3.1 Design constraints

3.1.1 Equilibrium Constraints

The first equilibrium constraint is the self-equilibrium condition of the initial prestress, which is described by Eq. (1). The second equilibrium constraint is the relation between the nodal loads and corresponding member forces, which is described by Eq. (3).

3.1.2 Member yielding and cable slackness constraints

The member stress must be within the allowable stress limit. In a tensegrity structure, cables and struts can be made of different materials and thus have different admissible stress limits, denoted as $\overline{\sigma}_c$ and $\overline{\sigma}_s$, respectively. Besides, since cables should always carry tension thus the stress of a cable should be always greater than zero. Note that the struts should be in compression in the *prestress state* but can be either in compression or tension in the *load state*. Use small positive values $\underline{\sigma}_c$ and $\underline{\sigma}_s$ to denote the absolute values of the minimum allowable stress of cables and struts respectively, then the member yielding and cable slackness condition can be expressed as

$$\sigma_i \in \begin{cases} \left[\underline{\sigma}_c, \overline{\sigma}_c\right], & \forall i \in C \\ \left.\begin{matrix} \left[-\overline{\sigma}_s, -\underline{\sigma}_s\right], & \text{under prestress state} \\ \left[-\overline{\sigma}_s, \overline{\sigma}_s\right], & \text{under load state} \end{matrix}\right\}, & \forall i \in S \\ 0, & \forall i \in N \end{cases} \tag{11}$$

where N is the set of members to be removed. Since the member types, i.e., C, S, N, are not predefined in a topology optimization procedure, constraint Eq. (11) cannot be expressed by only using the member internal force variables. To express the constraints mathematically and explicitly, vectors $\mathbf{s} \in \mathbb{R}^{m\times 1}$ and $\mathbf{c} \in \mathbb{R}^{m\times 1}$, whose entries are binary variables, are introduced here. By using variables **s** and **c** together with member force variable **F**, Eq. (11) can be re-expressed as

$$\begin{cases} -\overline{\sigma}_s a_i s_i + \underline{\sigma}_c a_i c_i \le F_i^0 \le -\underline{\sigma}_s a_i s_i + \overline{\sigma}_c a_i c_i \\ -\overline{\sigma}_s a_i s_i + \underline{\sigma}_c a_i c_i \le F_i^0 + F_i \le \overline{\sigma}_s a_i s_i + \overline{\sigma}_c a_i c_i \end{cases}, \quad \forall i \in E \tag{12}$$

Note that a member cannot be served as cable and strut simultaneously, variables **s** and **c** should satisfy the following constraint

$$s_i + c_i \le 1, \quad \forall i \in E \tag{13}$$

3.1.3 Strut buckling constraint

In addition to yielding, buckling is a critical issue that must be avoided for struts. This can be written as

$$-F_i^b \le F_i, \quad \forall i \in S \tag{14}$$

where F_i is the current internal force of strut *i* and F_i^b is the buckling load of strut *i* which mainly depends on the cross-section, length, and material property of the member. Without loss of generality, the Euler buckling load is considered in this study, i.e., F_i^b is given by

$$F_i^b = \frac{\pi^2 Y_i I_i}{l_i^2}, \quad \forall i \in S \tag{15}$$

where I_i is the moment of inertia of the cross-section.

It is known that for different cross-sectional forms, the moment of inertia has different expressions in terms of the cross-sectional dimensions. For the sake of simplification, steel tubes with circular hollow sections are adopted for struts in this study, and the thickness is assumed to be a specified ratio of the radius. In this case, the moment of inertia of the cross-section can be expressed as a function of the cross-sectional area, i.e.,

$$I_i = f\left(a_i\right), \quad \forall i \in S \tag{16}$$

thus Eq. (15) can be simplified to

$$F_i^b = \gamma_i a_i^2, \quad \forall i \in S \tag{17}$$

where γ_i is the coefficient determined by the length of strut *i*. Then Eq. (14) can be re-expressed as

$$-\gamma_i a_i^2 \le F_i, \quad \forall i \in E \tag{18}$$

Note that since *S* is unknown in advance, constraint Eq. (18) applies to all the candidate members in the optimization because for members to be served as cables or removed the constraint will be automatically satisfied.

3.1.4 Displacement constraint

To ensure the serviceability of the structure, the displacements of certain DOFs need to be kept within a limit. Denote the lower bound and upper bound for the i^{th} DOF as $\underline{u_i}$ and $\overline{u_i}$, respectively, then the displacement limit condition is expressed by

$$\underline{u_i} \le u_i \le \overline{u_i}, \quad \forall i \in D \tag{19}$$

where *D* denotes the set of the indices of the DOFs needed to be controlled.

3.1.5 Constraints for actuator layout and length changes

To mathematically describe the actuator layout eliminate E_a in Eq. (9), a vector $\boldsymbol{\chi} \in \mathbb{R}^{m\times 1}$ whose entries are binary variables, is introduced. The relation between and the actuator layout is defined as follows: if $\chi_i = 1$, it means that the i^{th} member is equipped with an actuator; if $\chi_i = 0$, it means the i^{th} member is not equipped with an actuator and serves as a passive member or to be removed.

Since only members equipped with actuators can actively change their lengths and the length change of an actuator cannot be too large and should be within a reasonable range, the member length change $\boldsymbol{\Delta L}$ and actuator layout variable $\boldsymbol{\chi}$ should satisfy the following relation

$$-\chi_i \Delta\overline{L} \le \Delta L_i \le \chi_i \Delta\overline{L}, \quad \forall i \in E \tag{20}$$

where $\Delta\overline{L}$ is the maximum length change of an actuator (shorten or lengthen). This constraint ensures that ΔL_i is zero if $\chi_i = 0$ and $\Delta L_i \in \left[-\Delta\overline{L}, \Delta\overline{L}\right]$ if $\chi_i = 1$. Besides, it might be needed to assign a lower and/or upper bound for the number of actuators, which can be simply realized by incorporating the following constraint

$$\underline{\chi} \le \sum_{i\in E} \chi_i \le \overline{\chi} \tag{21}$$

where $\underline{\chi}$ and $\overline{\chi}$ are the user-defined lower and upper bound for the number of the actuators. If a specified number of actuators is required, $\underline{\chi}$ and $\overline{\chi}$ can be set to the same as that value.

Since the actuator layout and member topology are coupled with each other, the relation between variables $\boldsymbol{\chi}$, **s**, and **c** should also be considered in the optimization, i.e.,

$$\chi_i \le s_i + c_i, \quad \forall i \in E \tag{22}$$

Without other constraints, the actuators can freely choose to be installed on either struts or cables. Considering the layout preferences, another two actuator layout modes :(1) all the actuators installed on struts, and (2) all the actuators installed on cables, can be adopted by replacing Eq. (22). The first mode can be realized by including the following constraints

$$\chi_i \le s_i, \quad \forall i \in E \tag{23}$$

Similarly, the second mode can be realized by including

$$\chi_i \le c_i, \qquad \forall i \in E \tag{24}$$

3.1.6 Constraints for structure mass and self-weight

When building the formulation of structure mass in the optimization model, the actuator mass cannot be constructed directly through Eq. (9). This is because the actuation force capacity of the actuators (i.e., F_i) is unknown in advance and the actuator index set E_a is also not predefined.

Since the actuation force capacity of an actuator relates to the maximum force that the corresponding member will carry, an auxiliary variable $\overline{F_i}$ is introduced here to approximate F_i . $\overline{F_i}$ is defined through the following constraint

$$-\overline{F_i} \le F_i \le \overline{F_i}, \qquad \forall i \in E \tag{25}$$

which means that $\overline{F_i}$ is an upper bound of the internal forces of member *i*. Therefore, $\overline{F_i}$ is also a lower bound of the actuator actuation force capacity if an actuator needs to be installed in member *i*. This way, F_i in Eqs. (9) and (10) can be replaced with $\overline{F_i}$ to express the mass of the actuators. Note that F_i in Eq. (25) denotes the current total internal force of member i: if there are no nodal loads and actuator control strategies apply to the structure, $F_i = F_i^0$, otherwise, $F_i = F_i^0 + F_i^e$ where F_i^e denotes the internal force of member *i* caused by the nodal loads and actuator length changes.

Through the definition of $\boldsymbol{\chi}$, it can be noticed that if member *i* is an active member, i.e., $\chi_i = 1$, then the mass of the corresponding actuator is $c\overline{F_i}\left(=c\chi_i\overline{F_i}\right)$; if member i is a passive member or to be removed, i.e., $\chi_i = 0$, then we can assume a virtual actuator with a zero mass is equipped in this member thus the corresponding actuator mass can also be expressed as $c\chi_i\overline{F_i}$. Therefore, by using the auxiliary variable $\overline{F_i}$ and the actuator layout variable $\boldsymbol{\chi}$, the mass of the actuators (i.e., Eq. (9)) can be re-expressed as

$$M_a = \sum_{i\in E} c\chi_i\overline{F_i} \tag{26}$$

Similarly, the self-weight applied to the i^{th} node Eq. (10) can be re-expressed as

$$W_i = \frac{1}{2}\left(\sum_{j\in E_i}\rho_j l_j a_j + c\sum_{j\in E_i}\chi_j\overline{F_j}\right)g \tag{27}$$

Then the self-weight load vector $\mathbf{P}^s$ can be constructed through Eq. (27).

3.1.7 Constraints for structure mass and self-weight

Considering the convenience of manufacturing and the availability of components in practical structure construction, some constraints can be enforced in the design.

(1) Lower and upper bounds for cross-sectional areas

To ensure the members used are commercially available, the cross-sectional areas of the members must be within a given range. This requirement is formulated into a constraint on the cross-sectional areas of members, i.e.,

$$\underline{a_s}s_i + \underline{a_c}c_i \le a_i \le \overline{a_s}s_i + \overline{a_c}c_i, \qquad \forall i \in E \tag{28}$$

where $\underline{a_c}$ and $\underline{a_s}$ are the lower bounds for the cross-sectional areas of cables and struts respectively; and $\overline{a_c}$ and $\overline{a_s}$ are the upper bounds for the cross-sectional areas of cables and struts respectively.

(2) Avoidance of member intersection

The existence of intersecting members may cause problems in manufacturing, hence the following constraint can be considered if necessary to avoid member intersection

$$s_i + s_{i'} + c_i + c_{i'} \le 1, \quad \forall \left(i, i'\right) \in E^{cross} \tag{29}$$

where E^{cross} collects the pairs of intersecting members in the ground structure.

(3) Actuator force capacity limit

The actuators available in practice may have an actuation force capacity limit, so in order to ensure that the forces carried by the actuators do not exceed the limit, the following constraint can be considered

$$\chi_i \overline{F_i} \le \overline{T}^{act}, \qquad \forall i \in E \tag{30}$$

where $\overline{T}^{act}$ is the actuation force capacity limit of available actuators.

3.2 Objective function

The total mass of the structure, i.e., Eq. (7), is adopted as the objective function, which is given by

$$M = M_m + M_a = \sum_{i \in E} \left(\rho_i l_i a_i + c \chi_i \overline{F_i} \right) \tag{31}$$

3.3 Optimization variables

In the formulated constraints and objective function, all the unknown parameters will be treated as optimization variables. The optimization variables can be divided into three types: design variables, state variables, and auxiliary variables. The design variables are independent structure parameters that determine the structure state; design variables include cross-sectional areas (i.e., assignment matrix **S**), member types (i.e., **s** and **c**), member prestress (i.e., $\mathbf{F}^0$), and actuator layout (i.e., $\boldsymbol{\chi}$) and length changes (i.e., ΔL). The state variables are parameters to describe the structure state and responses under the given design variables such as member forces and elastic elongations and nodal displacements caused by external loading. Auxiliary variables are variables that may have no explicit physical meaning but are introduced to better express some necessary constraints correctly and accurately, such as maximum member force $\overline{F}$.

4. Numerical Examples

A ground structure in Figure 1 is considered for topology optimization in this example. The positions of key nodes of the ground structure are from a Levy cable dome with a span of 50 m. The 145 candidate members in the ground structure contain all the members in the original Levy cable dome together with some additional members connecting some of the key nodes. All the DOFs of the surrounding nodes are fixed. Assume that a dead load of P_1 = 1.0 kN/m^2 is evenly distributed on the top of the structure. Two live loads are considered: the first live load P_2 = 0.5 kN/m^2 is full-span and evenly applied downward, and the second live load P_3 = 0.5 kN/m^2 is half-span and evenly applied downward. All the loads are equivalently transformed into nodal loads applied to the top of the structure. Three load cases as follows are considered in the optimization: (1) P_1, (2) $P_1 + P_2$, and (3) $P_1 + P_3$. No crossing members are allowed in the final optimized structure.

Assume that circular steel tubes and high-strength steel strands are used for struts and cables, respectively. The thickness of the circular steel tubes is assumed to be 10% of the radius. Struts and cables are assumed to have the same material density of 7.85 × 10^3/m^3 and Young's modulus of 206 GPa. The design strengths for steel tubes and high-strength steel strands are 310 MPa and 1260 MPa,

respectively. The lower bounds of stresses in members are set to 5% of the maximum allowable stresses, i.e., $\underline{\sigma}_c = 5\%\overline{\sigma}_c$ and $\underline{\sigma}_s = 5\%\overline{\sigma}_s$. The displacements of the loaded DOFs are required to be within a limit of span/250. The limit for the length changes of actuators is set to $\Delta\overline{L} = 250$ mm.

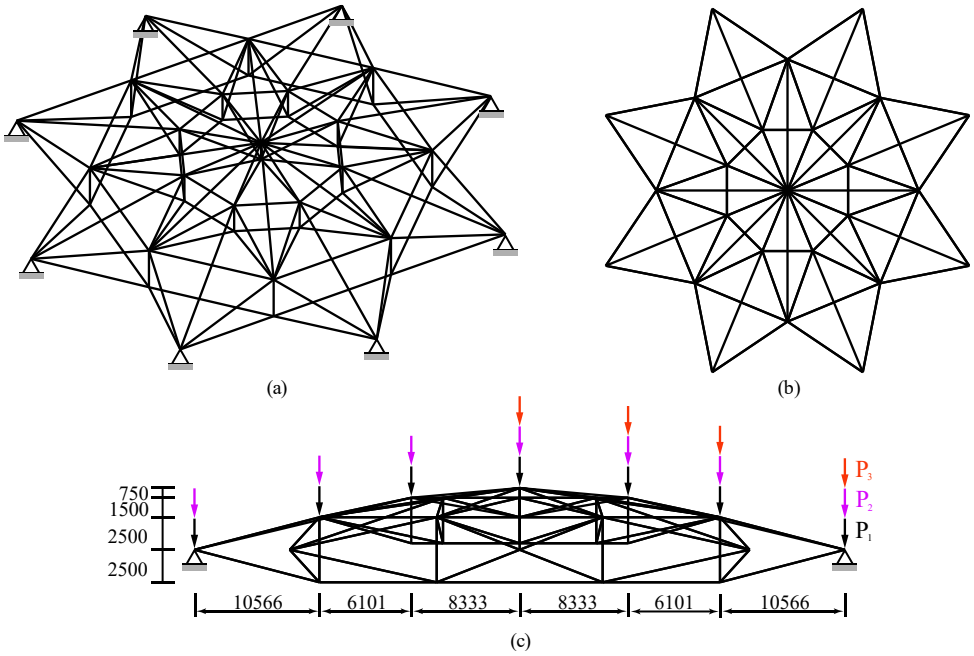

Figure 1 Ground structure for cable dome topology optimization

Firstly, the actuator layout is set to be able to be installed on both struts and cables and no limits are set for actuation force capacity. Solving the corresponding optimization model results in an optimized design shown in Figure 2(a). The structure has a total of 105 members consisting of 17 struts and 88 cables. It can be seen that all the struts on the bottom layer are installed with actuators. In addition, the eight circle cables on the second layer are also equipped with actuators. The maximum force carried by the actuators is 427.16 kN. The structure has a total mass of 5206.58 kg consisting of 4550.13 kg member and 656.45 kg actuator. Notably, stability check reveals that the structure has eight internal mechanism modes but all of them can be stiffened by the prestress and thus the structure is a prestress-stable system. For comparison, an active structure is also optimized based on the conventional Levy cable dome in which only the cross-sectional areas together with the actuator layout are treated as design variables. Figure 2(b) shows the optimized design. Since the member topology is fixed in the optimization, the obtained structure has 113 members consisting of 17 struts and 96 cables. The strut topology is identical to that in the previous design but the cable topology differs. In addition, 24 members including 16 struts and 8 cables are equipped with actuators, which is more than the previous topology-optimized design. The maximum force carried by the actuators is 420.12 kN. This active Levy cable dome has a total mass of 5456.66 kg consisting of 4966.91 kg member mass and 489.75 kg actuator mass. By comparing the two designs we can see that the optimized active structure through topology optimization achieves 4.58% smaller mass compared with the optimized active structure based on the conventional Levy cable dome.

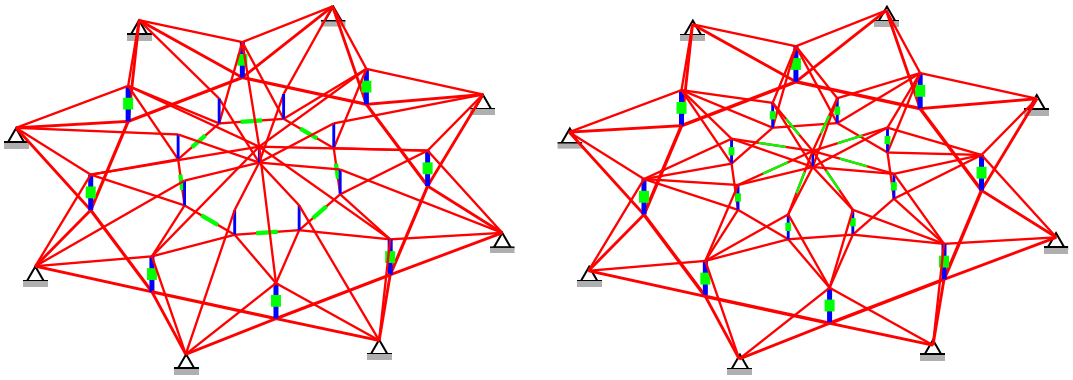

(a) (b)

Figure 2 Optimized active cable domes without considering actuator positions and actuation capacity limit: (a) topology-optimized design and (b) sizing-optimized design based on conventional Levy cable dome

Next, the actuator layout is set to be able to be installed on only struts, and the same two optimizations as mentioned above are carried out. Figure 3 shows the two obtained optimized structures. It can be seen that all the actuators are installed on the struts for both of the two optimized structures. The optimized design through topology optimization has a different member topology compared with the optimized design in Figure 2(a) and the structure is a kinematically determinate system without internal mechanism mode. Regarding the structure mass, the optimized design through topology optimization has a total mass of 5492.17 kg and the optimized active Levy cable dome has a mass of 5627.37 kg, which are both slightly higher than the corresponding designs allowing actuators to be installed on both cables and struts. The maximum forces carried by the actuators in the two structures are 428.12 kN and 430.97 kN, respectively. As can be seen, the maximum forces carried by the actuators in the four optimized designs are all above 400 kN.

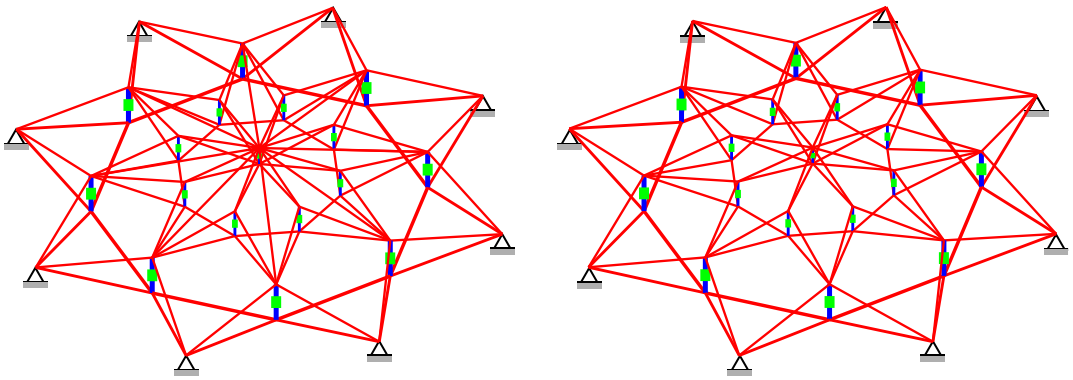

(a) (b)

Figure 3 Optimized active cable domes considering actuator positions but not considering actuation capacity limit: (a) topology-optimized design and (b) sizing-optimized design based on conventional Levy cable dome

Then, the actuator layout is still set to be able to be installed on only struts, and the actuation force capacity limit of actuators is set as 400 kN, then the same two optimizations as mentioned above are carried out. The obtained results are shown in Figure 4. As can be seen, for both of the two optimized structures, the actuators only distribute on the struts of the upper two layers, which is beneficial to reduce the maximum force carried by the actuators. In this way, the maximum forces carried by the actuators in the two structures are respectively only 102.63 kN and 169.05 kN, which significantly decreases compared to the previous two designs in Figure 3. However, the reduction of actuation forces leads to a significantly higher structure mass of 6326.83 kg and 6834.51 kg respectively for the two structures.

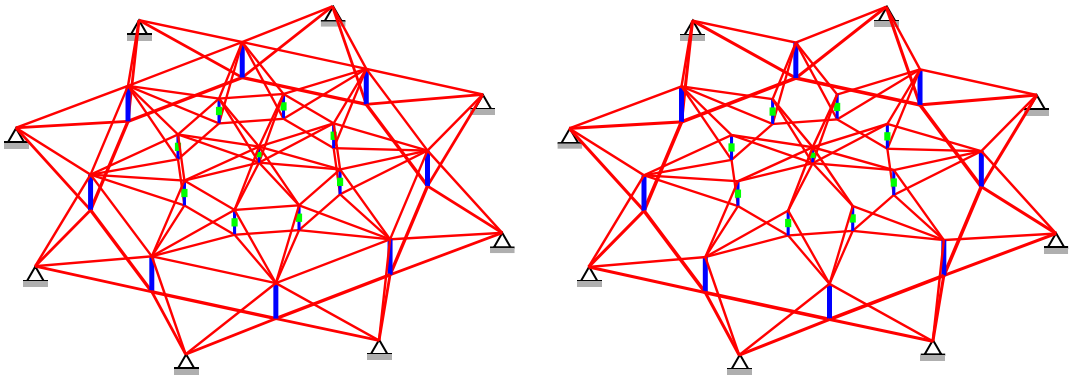

Figure 4 Optimized active cable domes considering actuator positions and actuation capacity limit: (a) topology-optimized design and (b) sizing-optimized design based on conventional Levy cable dome

5. Conclusions

This study proposes a general framework for the topology optimization of active tensegrity structures. Various design parameters, such as the actuator layout and actuator force capacity limit, are introduced in the optimization model, which allows to tune the design results according to practical design requirements and preferences. A cable dome example is employed to demonstrate the effectiveness of the proposed approach to design novel active structures with lighter weight.

Acknowledgements

This study is supported by the National Natural Science Foundation of China (Grant No. 52108182).

References

[1] K. Franklin, E. Ozkan, D. Powell, and others, "Design of the Kurilpa Pedestrian Bridge for Dynamic Effects Due to Pedestrian and Wind Loads," in *5th Civil Engineering Conference in the Asian Region and Australasian Structural Engineering Conference*, 2010, p. 885.

[2] D. H. Geiger, A. Stefaniuk, and D. Chen, "The design and construction of two cable domes for the Korean Olympics," in *Proceedings of the IASS symposium on shells, membranes and space frames*, 1986, vol. 2, pp. 265–272.

[3] C. Paul, F. J. Valero-Cuevas, and H. Lipson, "Design and control of tensegrity robots for locomotion," *IEEE Transactions on Robotics*, vol. 22, no. 5, pp. 944–957, 2006, DOI: 10.1109/TRO.2006.878980.

[4] K. Nagase and R. Skelton, "Minimal mass design of tensegrity structures," *Journal of the International Association for Shell and Spatial Structures*, vol. 55, no. 1, pp. 37–48, 2014.

[5] M. Chen and R. E. Skelton, "A general approach to minimal mass tensegrity," *Composite Structures*, p. 112454, 2020, DOI: 10.1016/j.compstruct.2020.112454.

[6] M. Chen, X. Bai, and R. E. Skelton, "Minimal mass design of clustered tensegrity structures," *Computer Methods in Applied Mechanics and Engineering*, vol. 404, p. 115832, 2023, DOI: 10/gs47q6.

[7] Y. Wang, X. Xu, and Y. Luo, "Minimal mass design of active tensegrity structures," *Engineering Structures*, vol. 234, p. 111965, 2021, DOI: 10.1016/j.engstruct.2021.111965.

[8] S. Pellegrino and C. R. Calladine, "Matrix analysis of statically and kinematically indeterminate frameworks," *International Journal of Solids and Structures*, vol. 22, no. 4, pp. 409–428, 1986, DOI: 10.1016/0020-7683(86)90014-4.

[9] C. R. Calladine and S. Pellegrino, "First-order infinitesimal mechanisms," *International Journal of Solids and Structures*, vol. 27, no. 4, pp. 505–515, Jan. 1991, DOI: 10.1016/0020-7683(91)90137-5.

[10] ENERPAC, "E328e Industrial Tools - Europe," 2016. [Online]. Available: https://www.enerpac.com/en-us/downloads. [Accessed: 28-Apr-2024].